

Charge sharing modeling in pixel detectors with capacitive charge division

J.Marczewski¹, D.Tomaszewski, K.Domanski, P.Grabiec
Institute of Electron Technology, Al. Lotnikow 32/46, Warszawa, POLAND
M.Caccia
Universita' degli Studi dell'Insubria and INFN, Via Valleggio 11, Como, ITALY
S.Borghi and R.Campagnolo
Universita' degli Studi di Milano and INFN, Via Celoria 16, Milano, ITALY
W.Kucewicz
University of Mining and Metallurgy, Al. Mickiewicza 30, Krakow, POLAND

Abstract

Pixel detectors with junctions interleaved to readout nodes have been modeled as an electrical network. Time domain analysis of a signal induced by an ionizing particle has been performed. Results are reported, together with a comparison to experimental data.

I. Introduction

Silicon detectors of ionizing radiation play a crucial role in High Energy Physics because of their excellent energy and space resolution, high efficiency and speed. One of present day challenges concerns spatial resolution improvements in hybrid pixel detectors, so far limited by the dimension of the electronics VLSI cell mating the pixel sensor. Recently the concept of improving the resolution by use of capacitive charge division between adjacent cells has been implemented in a pixel sensor [1]. In this novel configuration, only every n^{th} pixel is connected to the read-out electronics (Fig.1) and the charge generated by a particle passing underneath an interleaved pixel induces a signal on the capacitively coupled read-out pixels. In this layout, it is possible to implement a finer pitch for the same footprint of the VLSI chip mating the sensor and improve the spatial resolution. Prototypes of detectors with interleaved pixels have been designed and manufactured [2]. This paper summarizes the results of a time-dependent analysis of the signal in detectors with interleaved pixels, together with a simple steady-state model. The results have been compared to the measurements for a detector with implant width $60\mu\text{m}$, implant pitch $100\mu\text{m}$, readout pitch $200\mu\text{m}$. The comparison is based on the analysis of charge sharing and charge collection efficiency and its goal is

qualifying a tool for an optimization of the design parameters in future prototyping.

Charge sharing among neighboring read-out pixels is measured by the η function, defined as the signal amplitude on a reference pixel normalized to the total cluster pulse height. Charge collection efficiency is defined as the cluster pulse height for the generic impinging position of the particle normalized to its maximum value. The experimental results have been obtained scanning the detector backplane with an infrared (880nm) light spot; details of the measurements have been reported in [1].

II. Modeling of Capacitances

The capacitances required for the analysis have been calculated numerically and then compared to direct measurements. In these calculations, the detector was modeled as a 5×5 matrix of electrodes surrounded by a guard ring, facing a metal plane, specifying the pitch, the implant width and thickness of the detector according to the prototype. The capacitances have been obtained by Gauss law after solving the Laplace equation with suitable boundary conditions. The equation was solved with a finite element method using the OPERA-3D package [3]. The mesh required by the equation solver was optimized with respect to:

- the boundary conditions,
- requirement of the charge neutrality ,
- local strong variation of the electrical field.

Lower limits of the estimated pixel capacitances, due to the effect of having grad E variations on a scale smaller than the finest possible mesh for a 5×5 matrix, were evaluated recording the variations for different mesh scales. Upper limits of the estimated

¹ Corresponding author; e-mail address: jmarcz@ite.waw.pl

capacitances were computed replacing columns of pixels with plates of equal dimensions. The results of the two geometries were averaged and compared to the measurements, showing a fair agreement. The comparison and the breakdown of the different contributions to the total inter-pixel capacitance are shown in Table 1. The errors in the simulation are the sum in quadrature of the uncertainty resulting from the charge neutrality violation and the difference between the results of the two simulated geometries.

Measured C_{ip} [fF]	1038 ± 11
Calculated C_{ip} [fF]	880 ± 67
Measured C_{bp} [fF]	368 ± 5
Calculated C_{bp} [fF]	410 ± 90
Total C_{ip} [fF]	13.4 ± 0.9
C_{nn} [fF]	2.0 ± 0.1
C_{bp} [fF]	3.2 ± 0.7

Table 1. Upper part: inter-pixel (C_{ip}) and backplane (C_{bp}) capacitances values for 128 pixels in parallel. Lower part: single inter-pixel (C_{ip}), to the nearest neighbor pixel (C_{nn}) and backplane (C_{bp}) capacitance values. [1].

III. Time Dependent Charge Sharing Model

The pixel detector is represented by a net of cells. The basic elements of cells are shown in Fig.2, where G_{sub} and C_{sub} represents the admittance of the depleted silicon area and C_{cross} the inter-pixel capacitances. In order to make the figure more clear inter-pixel capacitances beyond the nearest neighbors are not marked, moreover, the interpixel conductances may be proven to be negligible.

The right-hand side pixel in the figure is read-out, connected via the oxide capacitance C_{ox} to the sense electronics, simply represented by a parallel G_{sense} - C_{sense} circuit; the read-out electronics not only integrates current flowing from the read-out pixels, but also keeps the DC voltage on its own input at the appropriate low level. It is not possible to approximate exactly its complex circuitry with passive R, C elements. Nevertheless this simple approximation (with a dedicated method of current integration) provides the necessary initial conditions for a proper circuit analysis.

The left-hand side pixel is close to a hypotetic charge release by an ionizing particle., originating a current pulse modeled according to the measurements reported in [4].

For every pixel, G_{gnd} represents a conductance of poly-Si resistor (see Fig.1), which biases the pixel and it is connected between the pixel and common ground.

The circuit analysis in the time domain has been done using the node-potential method, which consists in solving the set of linear equations expressing Kirchhoff's law for every node

$$\sum_l i_{k,l} = 0 \quad (1)$$

($k=1, \dots, n$; n – number of nodes)

where $i_{k,l}$ denotes current flowing through l^{th} path leading to k^{th} node and the sum is extended to all “branches” connected to k^{th} node.

In the equivalent circuit (Fig.2) of the detector three kinds of nodes may be distinguished:

1. nodes associated with interleaved pixels,
2. nodes associated with “read-out” pixels,
3. nodes associated with the input of sense electronics (separated by C_{ox} from node 2).

Ad.1.

For the nodes associated to interleaved pixels, the equation (1) may be written as follows:

$$\begin{aligned} & -G_{gnd} \cdot v_k(t) + G_{sub} \cdot (V_{sub} - v_k(t)) + \\ & + C_{sub} \cdot \frac{d}{dt}(V_{sub} - v_k(t)) + \\ & + \sum_l C_{cross,k,l} \cdot \frac{d}{dt}(v_l(t) - v_k(t)) = 0 \end{aligned} \quad (2)$$

If the pixel is hit by a particle the equation must be modified in order to take into account the additional current source.

Ad.2.

The equation (1) for the readout pixels may be written as follows:

$$\begin{aligned} & -G_{gnd} \cdot v_k(t) + G_{sub} \cdot (V_{sub} - v_k(t)) + \\ & + C_{sub} \cdot \frac{d}{dt}(V_{sub} - v_k(t)) + \\ & + \sum_l C_{cross,k,l} \cdot \frac{d}{dt}(v_l(t) - v_k(t)) + \\ & + C_{ox} \cdot \frac{d}{dt}(v_{k,sense}(t) - v_k(t)) = 0 \end{aligned} \quad (3)$$

where $v_{k,sense}(t)$ denotes potential at the input of the sense circuitry connected with k^{th} node. If the pixel is hit by a particle the equation must be modified in the same way as (2).

Ad.3.

For the nodes associated to the input of the readout electronics, the equation (1) may be written as follows:

$$\begin{aligned}
& -G_{sense} \cdot v_{k,sense}(t) - C_{sense} \cdot \frac{d}{dt} v_{k,sense}(t) + \\
& + C_{ox} \cdot \frac{d}{dt} (v_k(t) - v_{k,sense}(t)) = 0 \quad (4)
\end{aligned}$$

Equations (2), (3), (4) for $k=1, \dots, n$ are the set of linear equations, with initial conditions determined by the resistors. The initial potentials of pixel nodes are of the order of tenths of mV, whereas potentials of the sense nodes are zero volts. The resulting set of equations is solved using decomposition of the symmetric matrix of equations to lower and upper triangular matrices. The results comparing modeling with experimental studies are shown in Fig. 4 and 5.

The time dependent model has been used to estimate an influence of several factors on η and charge collection efficiency. An increase of bias resistance value from 5 to 20 MOhms causes an increase by 26% of the charge collection efficiency by the closest read-out node. An increase of inter-pixel capacitances by 50% enhances charge collection by 23% and the use of a thicker detector ($C_{sub}=2/3$ of the standard value) results by 11% increase of the efficiency. All these variations had little influence on η . The use in modeling the second order neighborhood had negligible influence on the results.

Calculated transients are shown in Fig.6. The read-out amplifier integrates only flowing-in current. The input of such an amplifier represents huge capacitive loading to each sense node. After the current flows-in (with the time constant of the same order as excitation) it reaches maximum and this value is latched-up by electronics. The transients show that there is no need for longer simulations than 100ns.

IV. Simple Charge Sharing Model

The use of the time dependent model is CPU time consuming, so a simple pure capacitance model suitable for the analysis of the steady-state conditions has been proposed. In this model only inter-pixel and backplane capacitances have been used; in such a case, the electrical neutrality condition for i^{th} node, surrounded by j^{th} nodes may be expressed as:

$$Q_i = \sum_{l=1}^k C_{i,j+l} \cdot (V_i - V_{j+l}) \quad (5)$$

where $Q_i = 0$ if the pixel is not hit.

The form of this equation is strictly the same as in the case of node potentials method, assuming a transformation from the (Q,C,V) domain to the (I,R,V) domain is performed. In such a case, equation (5) may be formally written as:

$$I = \sum_{l=1}^k \frac{1}{R_{i,j+l}} \cdot (V_i - V_{j+l}) \quad (6)$$

where $I=0$ in case the pixel is not hit. Equations in the form of (6) may be solved by standard tools like PSPICE, providing in an efficient way the information related to the steady state of the system. The results comparing modeling with experimental studies are shown in Fig. 4 and 5.

V. Discussion

The modeling is in an excellent agreement with charge sharing (η) experimental results. The charge collection efficiency studies show however that efficiency measured experimentally is higher than modeled. It may have resulted from the too big light spot size (estimated value 80 μm) compared to the pixel pitch. Another reason could have been the influence of a metallic grid evaporated on the detector backside to provide ohmic contact. Such a grid deflects light coming from backside in an uncontrolled way. Both reasons would have enhanced charge collection by read-out pixels in the case of the light spot being between them.

The use of our simple model gives nearly the same results as obtained by time dependent analysis. Slightly higher charge collection efficiency obtained in the case of the simple model may be understood as a lack of losses from resistive part of the network. However, the time dependent analysis is essential in the case of transient simulations or for the analysis of an influence of resistive components like bias resistors.

Conclusions

Two methods of charge sharing modeling have been developed and checked in the experimental way. These valuable tools may be used for optimization of future prototypes of hybrid sensors with interleaved pixels.

References

1. Characterisation of Hybrid Pixel Detectors ..., M.Caccia et al., Proc. of Linear Collider Workshop 2000 ,Fermi National Accelerator Laboratory, October 24-28, 2000 – to appear
2. W.Kucewicz et al., Acta Physica Polonica, **B30**, p. 2075 (1999)
3. OPERA-3D, software by Vector Fields Ltd., 24 Bankside, Kidlington, UK
4. R.Sonnenblick et al., Nuclear Instruments and Methods, **A310**, p.189 (1991)

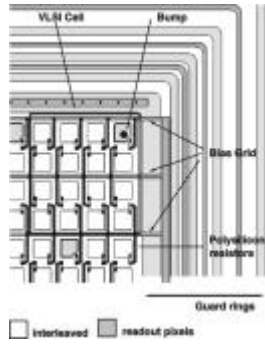


Fig. 1 Layout of a detector with interleaved pixels

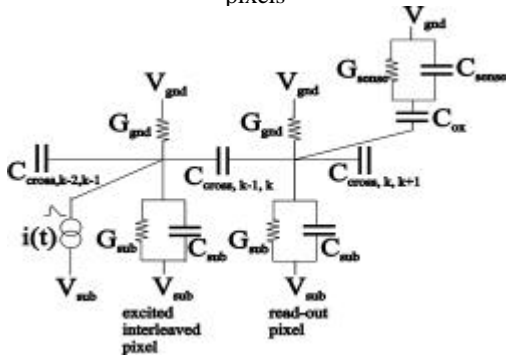


Fig. 2 Part of an equivalent circuit of the device. The meaning of symbols is explained in the text.

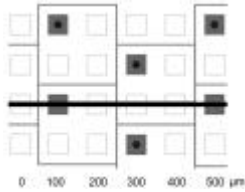


Fig. 3 Sketch of the tested detector. Dark pixels are read-out ones. The horizontal line identifies a scan with light spot. The frames indicate footprint of mating VLSI cells.

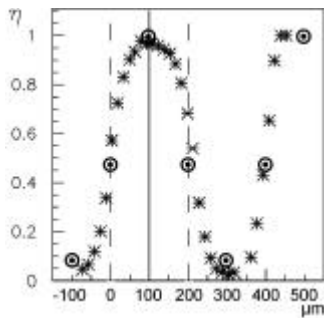


Fig. 4. The charge sharing among neighboring pixels. Horizontal scale as defined on Fig. 3. Vertical line shows the center of a reference pixel. The dashed lines – adjacent interleaved pixels. Stars from experiment. Circles from simulations (both models gave nearly the same results).

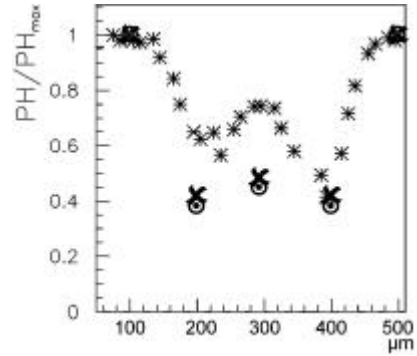


Fig. 5 Charge collection efficiency. Horizontal scale as defined on Fig. 3. Stars from experiment, circles from the time-dependent model. Crosses from simple model.

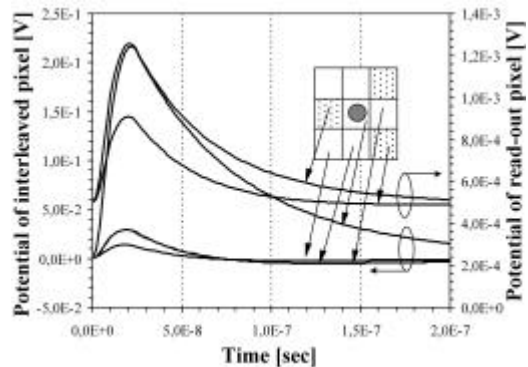
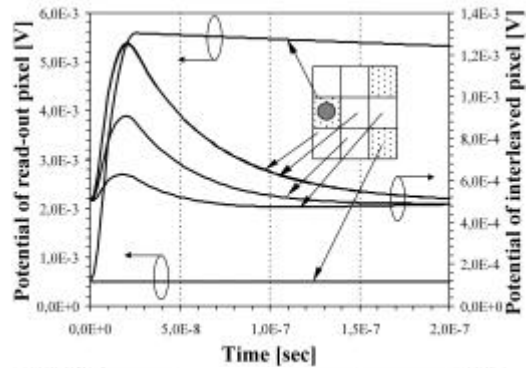


Fig. 6 Transients of potentials of interleaved and read-out (dotted) pixels after pulse of current spotted in position shown in inset.